

# A New Method to Investigate InGaAsP Single-Photon Avalanche Diodes Using a Digital Sampling Oscilloscope\*

Liu Wei<sup>†</sup>, Yang Fuhua, and Wu Meng

(State Key Laboratory for Superlattices and Microstructures, Institute of Semiconductors,  
Chinese Academy of Sciences, Beijing 100083, China)

**Abstract:** A near-infrared single-photon detection system is established by using pigtailed InGaAs/InP avalanche photodiodes. With a 50GHz digital sampling oscilloscope, the function and process of gated-mode (Geiger-mode) single-photon detection are intuitively demonstrated for the first time. The performance of the detector as a gated-mode single-photon counter at wavelengths of 1310 and 1550nm is investigated. At the operation temperature of 203K, a quantum efficiency of 52% with a dark count probability per gate of  $2.4 \times 10^{-3}$ , and a gate pulse repetition rate of 50kHz are obtained at 1550nm. The corresponding parameters are 43%,  $8.5 \times 10^{-3}$ , and 200kHz at 238K.

**Key words:** InGaAsP single-photon avalanche diode; 50GHz digital sampling oscilloscope; gated-mode

**EEACC:** 7230C

**CLC number:** TN312+.7

**Document code:** A

**Article ID:** 0253-4177(2006)10-1711-06

## 1 Introduction

The avalanche photodiode (APD) can be used as a single-photon detector because of its extremely high gain caused by avalanche breakdown. Therefore, only when reverse-biased beyond the breakdown voltage  $V_{\text{break}}$  can an APD be called a single photon avalanche diode (SPAD). Compared with photomultiplier tubes and Si or Ge SPADs, the ones with an InGaAs absorption layer extend the wavelengths into the near-infrared region. Actually, the InGaAsP SPAD can be adopted in any photon-starved detection field, such as eye-safe range finding, single molecule detection, and quantum key distribution systems<sup>[1]</sup>. There are three working modes for a SPAD: passive quenching, active quenching, and gated-mode (or Geiger mode)<sup>[2,3]</sup>. Considering the possibility of indicating the coming of photons by a pre-trig signal in most detection purposes, the gated-mode is a sound compromise between performance and complexity. Much attention has been paid to developing the gated-mode operation of InGaAsP SPADs<sup>[4~8]</sup>.

The avalanche breakdown itself cannot damage an APD, but the heat caused by the avalanche current is devastating. Hence a cryostat is a necessary integrated part of a SPAD. In this paper, we report a single-photon detector that is composed of an InGaAs/InP separated absorption and multiplication (SAM) APD<sup>[9]</sup> mounted in a specially designed liquid nitrogen cryostat with a steel vacuum shell around it to shield it from the environment. The single-photon signal and the bias are applied to the APD through a single mode fiber and SMA-type semi-rigid coaxial cables. The operation temperature of the APD can be changed from 77 to 323K with 0.1K step. Here it is limited within 203 to 273K, which is the domain of the Peltier cooler. The performance of our detector as a gated-mode single-photon counter is investigated by a 50GHz digital sampling oscilloscope and a 300MHz photon counter. To the best of our knowledge, this is the first time that a single-photon detection process has been illuminated besides the declared quantities. We also find that the calculated results can be influenced greatly by the counter's threshold.

Until now, most commercially available AP-

\* Project supported by the Special Funds for Major State Basic Research of China (No. 2001CB309300) and the Research Project of the Chinese Academy of Sciences

<sup>†</sup> Corresponding author. Email: liuw@semi.ac.cn

Received 31 March 2006, revised manuscript received 2 June 2006

DS are designed for the fiber optical communication. When used as SPADs, the breakdown voltage  $V_{\text{break}}$  and dark current of the APD are two key parameters to be considered. Table 1 summarizes some characteristics of one sample employed in this study.

Table 1 Characteristics of the APD (measured by authors)

Temperature/K	$V_{\text{break}}/\text{V}$ , Dark current/A	99% $V_{\text{break}}/\text{V}$ , Dark current/A
203	56.2, $1.3 \times 10^{-5}$	55.6, $4.9 \times 10^{-11}$
238	61.3, $1.6 \times 10^{-5}$	60.7, $1.8 \times 10^{-10}$

## 2 Experiment setup

Figure 1 shows a schematic of the setup for measuring the dark count probability per gate  $P_{\text{dark}}$ , the quantum detection efficiency  $\eta$ , and the gate pulse repetition rate  $1/\Delta t$ . The voltage pulse generator (I) acts as a timing controller. The voltage pulse generator (II) produces a single or double rectangular pulse with an amplitude of 5.1V and a full width at half maximum (FWHM)

of 4ns at a frequency of 10kHz, which act as the gate signal. The gate pulses are coupled with the DC bias through a bias tee offering the reverse bias of the APD. With proper adjustments, the reverse bias exceeds the breakdown voltage ( $V_{\text{break}}$ ) only within the gate time to make the APD work in a gated-mode that has sufficient sensitivity to be triggered by a single photon arriving at this time. The laser pulse generator can produce 1310 or 1550nm Gaussian pulses with a FWHM of 30ps (different laser heads). The laser pulses are attenuated to a single-photon energy level per pulse by a variable optical attenuator (25~85dB, 0.05dB per step). On the rising slope of the pre-trigger signals, the half-height point is chosen as the time reference point of the whole experimental system. There is a constant delay (about 74.625ns) between the reference point and the laser pulse. By disconnecting or connecting the optical fiber, the illumination of the APD can be turned off or turned on. The avalanche current is transformed into a voltage via a 50Ω grounded resistor.

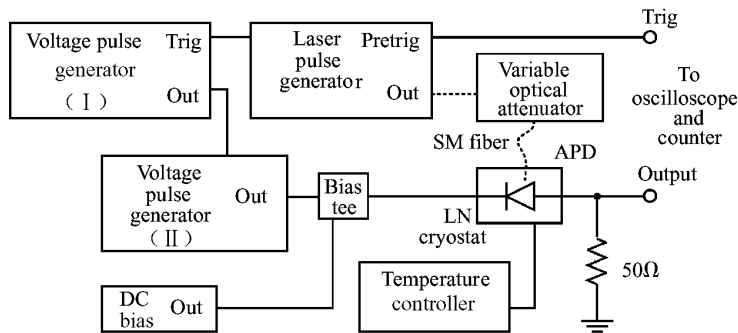


Fig. 1 Schematic diagram of the experiment setup to measure the dark count probability, quantum efficiency, and gate repetition rate of the gated-mode single-photon counter

## 3 Dark count probability and quantum efficiency

Figure 2 shows snapshots of the digital sampling oscilloscope, which demonstrate the characteristics of dark counts and the single-photon detection process. The reverse DC bias is 60V, and the temperature is 238K.

Before the avalanche breakdown, the APD acts like a capacitor. Therefore, the rising and falling edges of the rectangular voltage gate pulse

make the APD charge and discharge, respectively, leading to overshootings at the output port (see Fig. 2(a)). These overshootings indicate the time position of the gate.

It was assumed that there was no output when no photon arrived at the APD during the gate time. However, when highlighting the low probability events and using the database operation mode of the oscilloscope, in which the oscilloscope accumulates sampling points from different trigger cycles and shows them together on the display, from Fig. 2(a), we can see that a profile re-

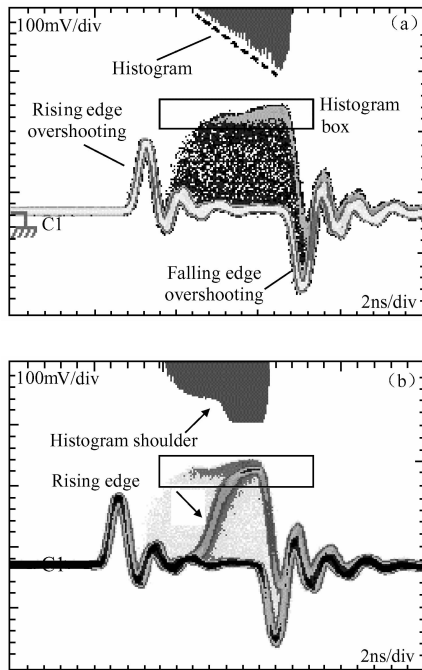


Fig.2 Outputs of the gated-mode single-photon detector at 238K and 60V DC bias (a) Horizontal histogram of the dark counts (line scale); (b) Avalanche outputs induced by single photons (logarithm scale)

sembling the shape of the voltage gate pulse is built. The amplitude of the profile is determined by the DC bias voltage, the amplitude of the gate, and the gate width. The dispersed sample points inside the profile come from one of two sources: the rising edge or the top of some avalanche pulses. This indicates the existence of avalanche pulses with different amplitudes and different FWHMs inside the profile. The reason arises from the randomness of the avalanche breakdown process<sup>[10]</sup>. These make it difficult to fix a proper threshold when using the counter. The pulse height distribution measurements confirm this judgment. All the pulses filling in the profile are called dark counts. In a SAM APD, dark counts mainly arise from the injection into the junction of charge carriers by thermal excitation and trapping center emission. The later effect also gives rise to afterpulses, in which the reemission of a charge trapped during an avalanche takes place and triggers a second avalanche breakdown in the subsequent gate pulse. In Fig. 2(a), the zero beginning of the horizontal histogram (numbers of the sampling points in the histogram box) indicates that the afterpulses are negligible under the 10kHz gate repetition rate. The linear increase of

the horizontal histogram (see the dotted line, linear scale) proves that the dark counts happen randomly within the gate time and are all quenched at the falling edge, which suggests a narrow voltage gate pulse leading to a small dark count probability. At the same time, a narrow gate means a good time resolution of the single-photon detector. However, one must notice that the amplitude of the dark counts will decrease as the gate time narrows due to the loss of high frequency components of the voltage gate pulses. This limitation comes mainly from the bandwidth of the single-photon detector. It is essential that the amplitude of the dark counts exceeds the amplitude of the leading edge overshootings, at least at the point of the periphery counting instrument's view, to pick up the right avalanche outputs. This is just the method we use in this experiment. In fact, besides this, another effect can be utilized. There are two falling edge overshootings with different amplitudes in Fig. 2(a), which are more obvious in Fig. 2(b). When an avalanche is triggered, the APD's resistance becomes very small, so the RC time of the detector and then the falling edge overshootings almost disappear. The avalanche outputs can be distinguished even with a gate width of hundreds of picoseconds<sup>[11]</sup>. However, this requires a much higher-resolution counting instrument to measure the difference.

Figure 2(b) shows the avalanche outputs by tuning the delay of the voltage pulse generator ( $I$ ) to achieve the time alignment between the voltage gates and the laser pulses. The optical attenuator is set to 72dB. The mean photon number  $n$  per laser pulse is 0.3. Comparing it with Fig. 2(a), we see that a leading edge extrudes from the disorder dark count background. The shoulder of the histogram (log scale) indicates a great increase of the avalanche output pulse quantity. The clearer profile represents the light counts, which are the sum of dark counts and photon counts. The photon counts act the same as the dark counts except for their much greater probability and the confinement of their leading edge time position. (According to the 4ns gate width, the jitter caused by the 30ps FWHM of the laser pulses is negligible.)

Using a 300MHz counter, we measure the dark count probability per pulse  $P_{\text{dark}}$  and the light

count probability  $P_{\text{light}}$ . Taking the Poisson statistics of the number of photons per pulse into account, the quantum efficiency  $\eta$  can be estimated by the equation  $P_{\text{light}} = 1 - (1 - P_{\text{dark}})e^{-n\eta}$  (see Ref. [8]). Figure 3 shows the dependence of  $P_{\text{light}}$  on the mean photon number  $n$  per pulse at 1550nm. The DC bias is 99%  $V_{\text{break}}$ , and the gate voltage is 5.1V. The open circles represent the measured values at 238K with a dark count probability  $P_{\text{dark}} = 1.0 \times 10^{-2}$  while the dash dot line corresponds to a curve fit, yielding a quantum efficiency  $\eta = 43.4\%$ . The open triangles and the solid line give  $\eta = 51.9\%$  with  $P_{\text{dark}} = 2.45 \times 10^{-3}$  at 203K. Figure 4 shows the dark count probability  $P_{\text{dark}}$  versus quantum efficiency  $\eta$  measured against the DC bias voltage from 96%  $V_{\text{break}}$  to 99%  $V_{\text{break}}$  at 238K (open circles) and 203K (open triangles), respectively, with a fixed threshold of 90mV. The dashed lines are a fit to guide the eye. At 203K, the quantum efficiency increases quickly but the dark count probability increases very slowly compared to 238K. Both Figures 3 and 4 verify that cooling the detector can reduce the dark counts and enhance the quantum efficiency. This can be explained by the low thermal generation and the long free path of the charges in the depletion region. The dark current of the APD is the key factor. An APD with a low dark current level will need little cooling and yield a small dark count probability and quantum efficiency, and vice versa<sup>[12]</sup>. However, a positive temperature coefficient of the avalanche breakdown and the tunneling will limit the further effect of cooling.

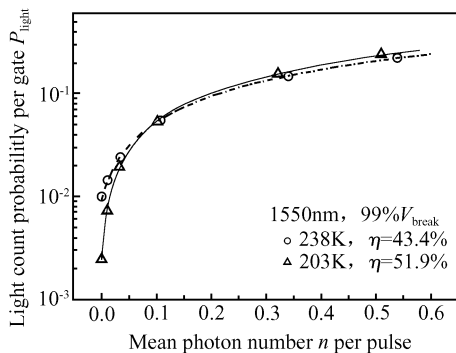


Fig. 3 Light count probability  $P_{\text{light}}$  as a function of mean photon number  $n$  per pulse

The threshold level of the counter can also influence the dark counts and quantum efficiency due to the randomness of the avalanche break-

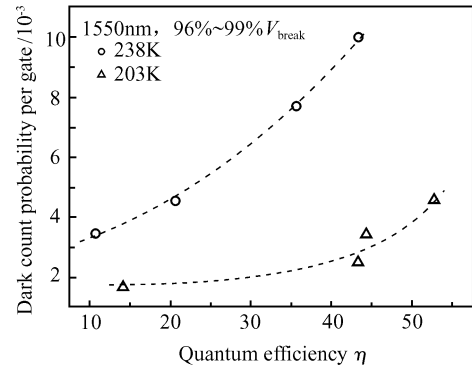


Fig. 4 Dark count probability per gate versus quantum efficiency  $\eta$

down (both beginning time and amplitude). For instance, at 203K and 99%  $V_{\text{break}}$ , the quantum efficiency is almost equal but the dark count probability is half when choosing 130mV instead of 90mV as the threshold. A higher threshold can be adopted in a higher bias region to reduce the dark count probability, and a lower one to increase the light counts in a low bias region. In this work, we find that the margin of the threshold is less than 10mV. Therefore it should be considered carefully for repeated measurements.

When the wavelength of the single photon is 1310nm, the quantum efficiency is 10% to 20% bigger. This can be explained by the different absorption coefficients of the InGaAs material<sup>[13]</sup>.

## 4 Gate repetition rate

The gate repetition rate represents how fast a single-photon detector can work. It is the reciprocal of the time interval  $\Delta t$  between two sequential gates. In this paper, we defined it as the case in which the afterpulse count probability is lower than the thermal excitation dark count probability. However, it is not necessary that the single-photon detector always run at a frequency below  $1/\Delta t$ , as in the case of quantum key distribution, for instance<sup>[14,15]</sup>. Figure 5 shows the afterpulse effect measured with the double-gate method. The time interval  $\Delta t$  is 8ns. The DC bias and gate voltage are 60 and 5.1V at 238K. The two peaks of the vertical histogram representing afterpulse counts and the absence of an avalanche almost have the same amplitude, which indicates a 50% afterpulse count probability per gate. Figure 6 is the measured dependence of the afterpulse count

probability on the interval  $\Delta t$  at 238K. According to the criteria described above, it yields a  $\Delta t$  of about  $5\mu\text{s}$ , or a gate repetition rate of 200kHz. The afterpulse counts decrease greatly within  $1\mu\text{s}$ . At 203K, the result is about  $20\mu\text{s}$ , and then 50kHz.

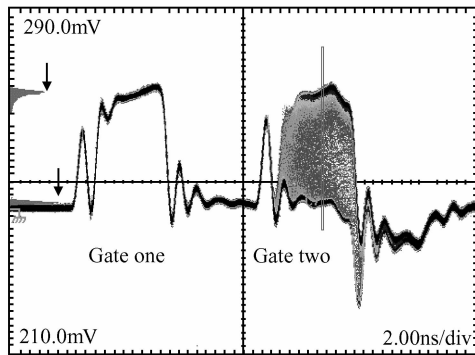


Fig. 5 Afterpulses

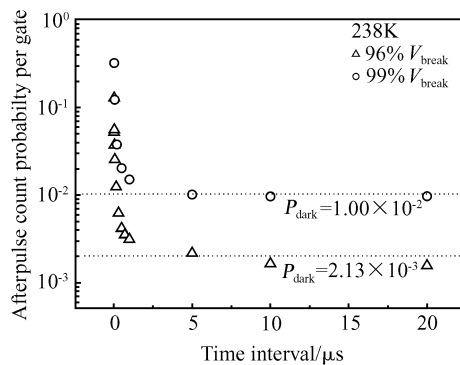


Fig. 6 Afterpulse count probability per gate versus time interval. The thermal excitation dark count probability per gate is represented by the horizontal dotted lines.

The afterpulses are proportional to the number of filled traps and the emission lifetime of the carriers from the trapping levels, which are related to voltage bias and operation temperature, respectively. A higher voltage bias will lead to a larger charge flow, and then a higher number of carriers trapped. Because of the limitation of our instruments, the dynamic range of the gate height to the DC bias ratio is small. The Franz-Keldish effect is not obvious in Fig. 6 (see Ref. [5]). The emission lifetime increases exponentially with the reduction in temperature. A much longer  $\Delta t$  is needed when working at low temperatures. It is necessary to find an optimized point between low dark count probability and high speed.

## 5 Conclusions

A single-photon detection system using InGaAsP avalanche photodiodes is established. The performance of the detector working under gated-mode is investigated with a simple method using a digital sampling oscilloscope and a counter. From one sample, at the operation temperature of 203K, we achieved a quantum efficiency of 52% with a dark count probability per gate of  $2.4 \times 10^{-3}$ , and a gate pulse repetition rate of 50kHz at a wavelength of 1550nm. The corresponding parameters are 43%,  $8.5 \times 10^{-3}$ , and 200kHz at 238K. The quantum efficiency obtained here is superior to others (see Ref. [8]), but the dark count probability is degenerated because of the high level dark current of the APD used in this experiment. Nevertheless, our detector can fulfill the requirements of diverse applications compared with some commercially available ones (dark counts:  $500 \sim 2000\text{s}^{-1}$ ).

Besides the bias, the performance can be greatly influenced by gate width, repetition rate, temperature, and the threshold of the detector. Despite the trade-off relationships among these parameters, they offer more freedom depending on the applications.

## References

- [1] Karlsson A, Bourennane M, Ribordy G, et al. A single-photon counter for long-haul telecom. *IEEE Circuits and Devices Magazine*, 1999, 15(6):34
- [2] Liang Chuang, Liao Jing, Liang Bing, et al. Performance of a silicon avalanche diode as a single photon detector. *Acta Photonica Sinica*, 2000, 29(12):1142 (in Chinese) [梁创, 廖静, 梁冰, 等. 硅雪崩光电二极管单光子探测器. *光子学报*, 2000, 29(12):1142]
- [3] Zappa F, Ghioni M, Cova S, et al. An integrated active-quenching circuit for single-photon avalanche diodes. *IEEE Trans Instrumentation and Measurement*, 2000, 49(6):1167
- [4] Levine B F, Bethea C G. Single photon detection at  $1.3\mu\text{m}$  using a gated avalanche photodiode. *Appl Phys Lett*, 1984, 44(5):553
- [5] Lacaita A, Zappa F, Cova S, et al. Single-photon detection beyond  $1\mu\text{m}$ : performance of commercially available InGaAs/InP detectors. *Appl Opt*, 1996, 35(16):2986
- [6] Ribordy G, Gautier J D, Zbinden H, et al. Performance of InGaAs/InP avalanche photodiodes as gated-mode photon counters. *Appl Opt*, 1998, 37(12):2272
- [7] Stucki D, Ribordy G, Stefanov A, et al. Photon counting for quantum key distribution with Peltier cooled InGaAs/InP APD's. *Quant-ph/0106007*, 2001:1

- [8] Yoshizawa A, Tsuchida H. A 1550nm single-photon detector using a thermoelectrically cooled InGaAs avalanche photodiode. *Jpn J Appl Phys*, 2001, 40:200
- [9] Ito M, Mikawa T, Osamu W. Optimum design of  $\delta$ -doped InGaAs avalanche photodiode by using quasi-ionization rates. *J Lightwave Technol*, 1990, 8(7):1046
- [10] Todd C D. Zener and avalanche diodes. USA: Wiley-Interscience, 1977:7
- [11] Yoshizawa A, Kaji R, Tsuchida H. Gated-mode single-photon detection at 1550nm by discharge pulse counting. *Appl Phys Lett*, 2004, 84(18):3606
- [12] Liu Wei, Zeng Yuxin, Yang Fuhua, et al. A gated-mode single-photon detection system for quantum key distribution using InGaAs avalanche photodiodes. ERATO Conference on Quantum Information Science, Kyoto, Japan, 2003:99
- [13] Humpherys D A, King R J, Jenkins D, et al. Measurement of absorption of  $\text{In}_{0.53}\text{Ga}_{0.47}\text{As}$  over the wavelength ranger 1.0 ~ 1.7 $\mu\text{m}$ . *Electron Lett*, 1985, 21:1187
- [14] Yoshizawa A, Kaji R, Tsuchida H. A method discarding after-pulses in single-photon detection for quantum key distribution. *Jpn J Appl Phys*, 2002, 41:6016
- [15] Yoshizawa A, Kaji R, Tsuchida H. After-pulse-discarding in single-photon detection to reduce bit errors in quantum key distribution. *Optics Express*, 2003, 11(11):1303

## 基于数字采样示波器的 InGaAsP 单光子雪崩二极管的特性\*

刘 伟<sup>†</sup> 杨富华 吴 孟

(中国科学院半导体研究所 超晶格国家重点实验室, 北京 100083)

**摘要:** 介绍了由带尾纤的 InGaAs/InP 雪崩光电二极管建立的近红外单光子探测系统. 使用带宽 50GHz 的数字采样示波器, 首次直观地展现了门模式(即盖革模式)工作状态下, 单光子探测的模式和过程. 并且在波长分别为 1310 和 1550nm 的情况下进行了定量研究. 在 1550nm, 工作温度 203K 条件下, 该探测器达到了暗计数概率  $2.4 \times 10^{-3}$  每门, 量子效率 52%, 50kHz 的门信号重复频率; 在工作温度为 238K 时, 相应参数分别为  $8.5 \times 10^{-3}$ , 43% 和 200kHz.

**关键词:** InGaAsP 单光子雪崩二极管; 50GHz 数字采样示波器; 门模式

EEACC: 7230C

中图分类号: TN312+.7

文献标识码: A

文章编号: 0253-4177(2006)10-1711-06

\* 国家重点基础研究专项基金(批准号:2001CB309300)和中国科学院研究计划资助项目

<sup>†</sup> 通信作者. Email: liuw@semi.ac.cn

2006-03-31 收到, 2006-06-02 定稿